

# Modelling of Pd-membranes deformation during hydrogen separation

Artem Pilipenko  
SINTEF Materials & Chemistry, Oslo

## Abstract

Pd-membranes used for hydrogen separation work at elevated temperatures under pressure causing plastic deformation of the membranes. The problem is complicated by the fact that these membranes are very thin. Preferable thickness varies between 1 and 5 $\mu\text{m}$ . Different mathematical approaches can be used for modelling of this complex situation. Variety of 2D and 3D ABAQUS models are tested for this purpose. To simulate interface between the membrane and substrate, some models include contact analysis. Results from different models have been compared. The 2D-axisymmetric model is recommended for further inverse modelling due to its robustness and appropriate approximation of the real phenomenon. This model takes into account the through-thickness distribution of the stress-strain fields which in its turn is important for the accurate prediction of the membrane deformation under pressure.

## 1. Introduction

The main aim of this investigation has been to focus on thermo-mechanical problems in Pd-membranes deformation during hydrogen separation. Hydrogen separation is an important stage of some technological processes, such as hydrogen production and power generation [1,2]. Principles of the process are outlined in Figure 1. The process takes place in four steps as

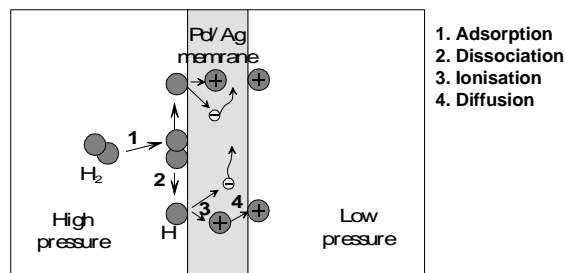


Figure 1. Scheme of hydrogen permeation through a Pd/Ag membrane. Four reactions are involved.

Hydrogen and oxygen are combined in a fuel cell to produce electrical energy. It can produce electrical energy with high efficiency. The only product of such reaction is water, so locally it is pollution-free.

A proton exchange membrane (PEM) fuel-cell requires pure  $\text{H}_2$  (less than 20ppm CO) for operation [3]. The high purity can be obtained using Pd membranes for production of  $\text{H}_2$ .

Molecules of hydrogen adsorb on the palladium surface. The molecules then dissociate at the gas-anode interface and incorporate into the material of the membrane. The next stage is diffusion of the hydrogen atoms through the bulk of Pd/Ag membrane [4,5].

The flux of hydrogen is proportional to the partial pressure of  $\text{H}_2$  in the gas mixture and inversely proportional to the thickness of the membrane. In other words, to reach the highest flux through the membrane we need to have a very thin membrane able to withstand high pressure of gas. Finite element modelling can be a helpful instrument for prediction of the membrane deformation.

The work on evaluation of different modelling techniques as applied to deformation of thin membranes under pressure has been done in order to define the type of modelling that can be used for further determination of mechanical properties. The mechanical properties of thin membranes can be determined based on inverse modelling of the deformation process.

The most critical part of the inverse modelling is correctly simulated deflection of the membrane that can be further compared to deformation of the real membrane withstanding pressure load.

## 2. Physical phenomenon and its model

Pd-membranes used for hydrogen separation work at elevated temperatures under pressure. This causes both elastic and plastic deformation of the membranes as discussed below.

The membrane itself is placed on the porous substrate with variable pore-size inside the reactor. To complicate the situation, the membrane expands due to increasing temperature and increasing hydrogen content inside the membrane.

Several simplifications are made to model this complicated physical phenomenon (illustrated in Figure 2). The simplifications currently used are:

1. The model is limited to one (a few) pore of characteristic dimension and simplified shape (circular);
2. It is assumed that Pd-membrane has a constant thickness;
3. The process of loading is isothermal, i.e. no temperature dependence is taken into account;
4. Pd-membrane expansion due to hydrogen content is not taken into account;
5. Porous substrate is assumed to be a rigid body.

A more realistic approach is to eliminate the simplification number 3 and 4. Then the actual expansion of the membrane due to increasing temperature and hydrogen pickup are accounted for.

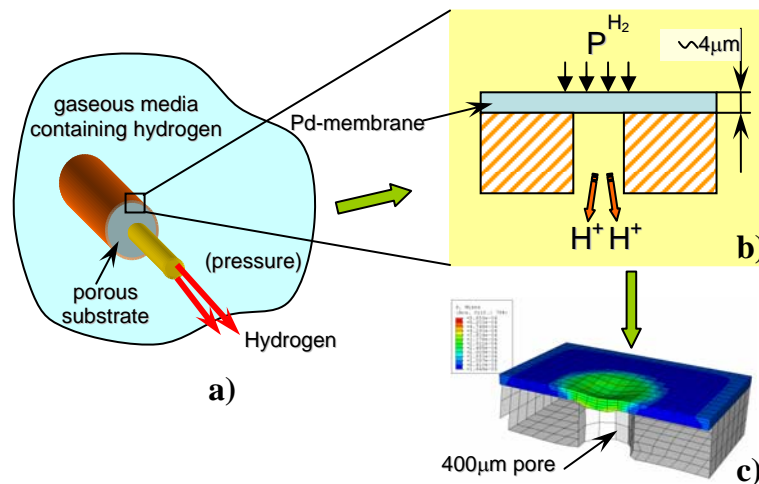


Figure 2. Example of modelling of the Pd-membrane under pressure; (a) – physical phenomenon; (b) – localisation; (c) – 3D model of the working membrane.

### 2.1 Geometry and material properties

For interrogation of the models the following dimensions of the membrane and porous substrate have been chosen:

- Membrane thickness  $t^{mebr}=0.004\text{mm}$  ( $4\mu\text{m}$ )
- Diameter of the holes in the substrate  $D^{hole}=0.4\text{mm}$  ( $400\mu\text{m}$ )

The Pd-membrane studied in this article has the composition 77%Pd and 23%Ag. The membrane is made of a very fine-grained material with the following properties:

- Density  $\rho=12.013\text{g/mm}^3$ ;
- Elasticity modulus  $E=200.000\text{ N/mm}^2$  (200GPa);
- Poisson's coefficient  $\nu=0.34$ ;
- Yield stress  $\sigma^Y=1500\text{ N/mm}^2$  (1.5GPa) at plastic deformation  $\epsilon^{pl}=0$ ;
- Yield stress  $\sigma^Y=1800\text{ N/mm}^2$  (1.8GPa) at plastic deformation  $\epsilon^{pl}=0.1$ , assuming isotropic hardening.

These material properties, especially the ones characterising the inelastic deformation, are subjected to further revision and change because they are not investigated and reported enough for the investigated material.

### 3. A survey of tested models

#### 3.1 2D model, deformable body is modelled as a wire

Deformation of the Pd-membrane can be simulated in a simplest way by a 2D model where the membrane is approximated by the 2-node linear axisymmetric shell elements **SAX1**. The scheme of the model is shown in Figure 3. The perforated substrate is defined as an analytical rigid body.

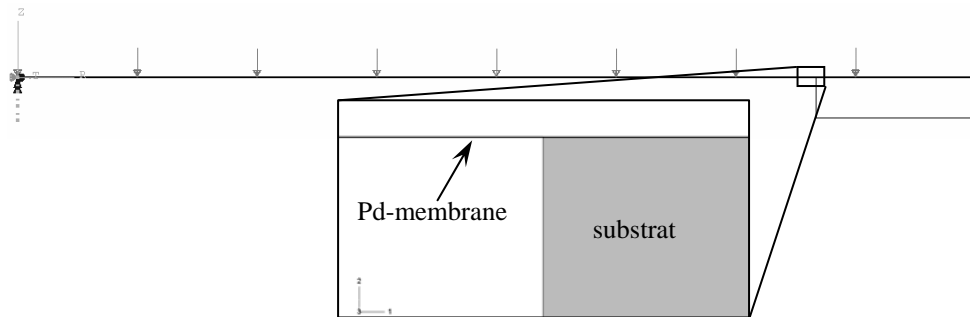


Figure 3. Scheme of 2D model; Pd-membrane is modelled as a wire.

The gas pressure is simulated by the distributed pressure applied to one side of the membrane and assigned in Figure 3 by arrows. Mechanical contact between the membrane and the substrate can be specified as non-frictional tangential behaviour or as tied, depending on the necessity. The normal behaviour is specified as a hard contact allowing separation after the contact.

#### 3.2 2D axisymmetric model

Deformation of the Pd-membrane can also be simulated by a 2D model where the membrane is approximated by the 4-node bilinear axisymmetric solid elements **CAX4**. The scheme of the model is shown in Figure 4. The perforated substrate is defined as an analytical rigid body.

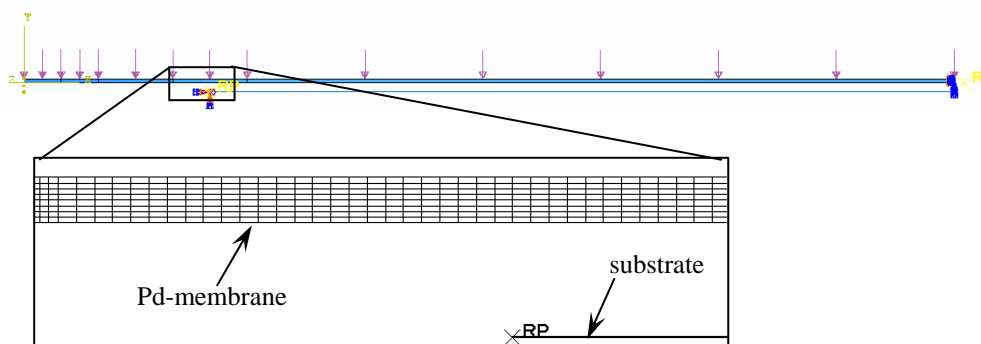


Figure 4. Scheme of 2D axisymmetric model.

Mechanical contact between the membrane and the substrate is specified in similar way as described above for the previous model (Figure 3).

### 3.3 3D model, deformable body is modelled as a shell

Deformation of the Pd-membrane can also be simulated by a 3D model where the membrane is approximated by the 4-node doubly curved general-purpose shell elements **S4**. The scheme of the model is shown in Figure 5. In this scheme three sizes of the pores are tested simultaneously. The perforated substrate is simulated by applying **ENCASTRE** boundary conditions to the edges of the membrane. Such simplification can be used if the membrane is perfectly glued to the porous substrate.

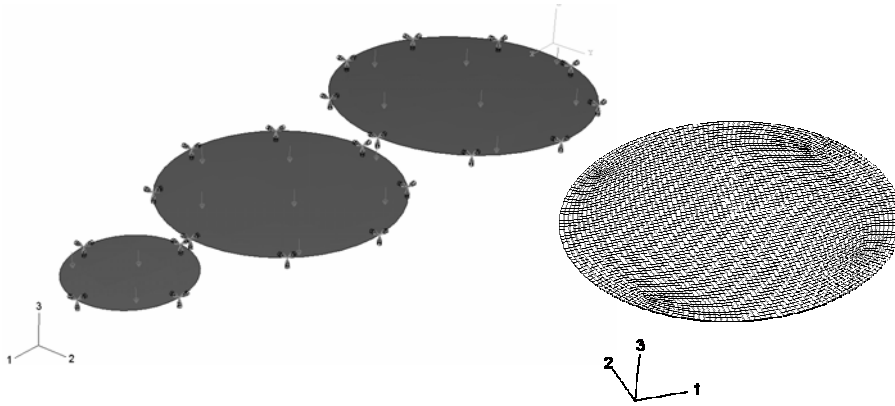


Figure 5. Scheme of 3D model; Pd-membrane is modelled as a shell.

### 3.4 3D model including contact analysis, deformable body is modelled as a shell

Deformation of the Pd-membrane can also be simulated by a 3D model where the membrane is approximated by the 4-node doubly curved general-purpose shell elements **S4**. The scheme of the model is shown in Figure 6. The perforated substrate is defined as a discrete rigid body.

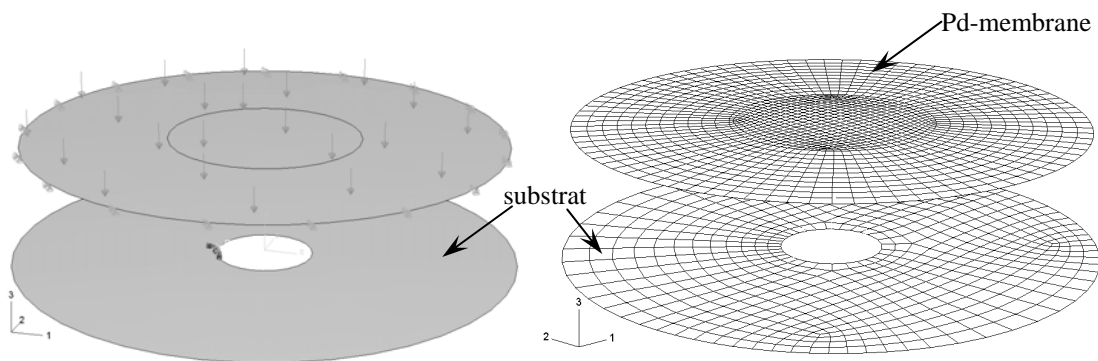


Figure 6. Scheme of 3D model including contact analysis; Pd-membrane is modelled as a shell.

Mechanical contact between the membrane and the substrate is specified in similar way as described in section 3.1. Such approach allows us to model friction between the membrane and substrate, although the solution of this model is more time consuming as compared to the model described in section 3.3. This is due to involvement of the contact analysis and significant increase of the number of elements. The number of elements has grown because in this model not only the 400 $\mu\text{m}$  in diameter deforming membrane is meshed. The deforming membrane and the adjacent area, 1000 $\mu\text{m}$  in diameter, are included in the model.

The contact bodies are initially separated due to peculiarity of the **ABAQUS** contact analysis. During the first time step the membrane is moved closer to the substrate with the hole, leaving a 0.1 $\mu\text{m}$  gap between the

bodies. The outer edge of the adjacent area is being totally constrained after that. During the second time step the pressure is applied to the top surface of the membrane, first bringing the two bodies in contact and later deforming the membrane that has no support of the substrate (centre of the membrane).

### 3.5 Full scale 3D model

Deformation of the Pd-membrane can also be simulated by a 3D model where the Pd-membrane is approximated by the 8-node linear brick elements **C3D8**. The scheme of the model is shown in Figure 7. The perforated substrate is defined as a discrete rigid body. Such approach allows us to model friction between the Pd-membrane and substrate.

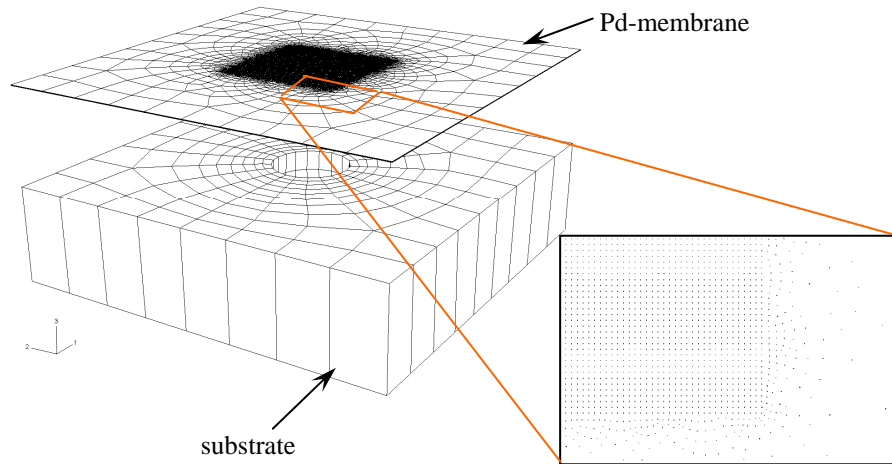


Figure 7. Scheme of 3D model including contact analysis.

This model has fewer approximations compared to the other models due to its full-dimensionality. It also brings complications such as significantly increasing number of elements. The model with highest mesh density consists of more than 125,000 elements. The membrane itself is only 4 $\mu\text{m}$  thick, while its modelled part is 1000 $\mu\text{m}$  in the other two dimensions. The shape of the used brick elements should be kept as close to cubic shape as possible. Otherwise the predicted deformation of the membrane would be underestimated.

### 3.6 Analytical solution

There is an analytical solution describing deformation of the circular membrane under load [6]. This solution is valid for elastic loading only:

$$w = \frac{q}{64D} (a^2 - r^2)^2,$$

where  $w$  is deflection;  $q$  is intensity of load (distributed load);  $r$  is distance;  $a$  is radius of the membrane;  $D$  is flexural rigidity of the plate:

$$D = \frac{Eh^3}{12(1-\nu^2)},$$

where  $h$  is membrane thickness;  $E$  is elasticity modulus and  $\nu$  is Poisson's ratio.

This solution can be used for testing ABAQUS model within the elastic part of loading.

## 4. Results and discussion

### 4.1 Comparison of the models (both elastic and plastic deformation)

The simulated Mises stress distribution [7] is shown for the case of 15bar (1.5MPa) pressure applied to the top surface of the membrane in Figure 8. These results are from the model where the membrane is modelled by the shell elements (section 3.3).

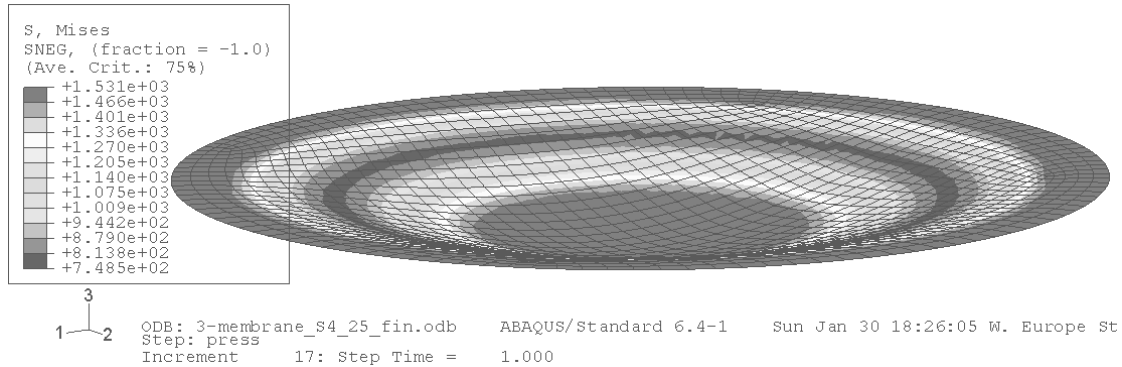


Figure 8. Mises stress distribution.

The whole membrane is stretched due to applied pressure. Along the radius Mises stress varies between 750MPa and 1530MPa. Maximum is reached in the centre region and in the region close to the edge of the membrane. Logically, in these regions the most plastic deformation occurs (see Figure 9). It allows us to conclude that the initial rupture of the membrane can take place either in the centre or at the edge. These locations are competitive because the centre has a wider region that undergoes plastic deformation, while the edge in real life is in direct contact with possible stress concentrator (edge of the hole in the substrate).

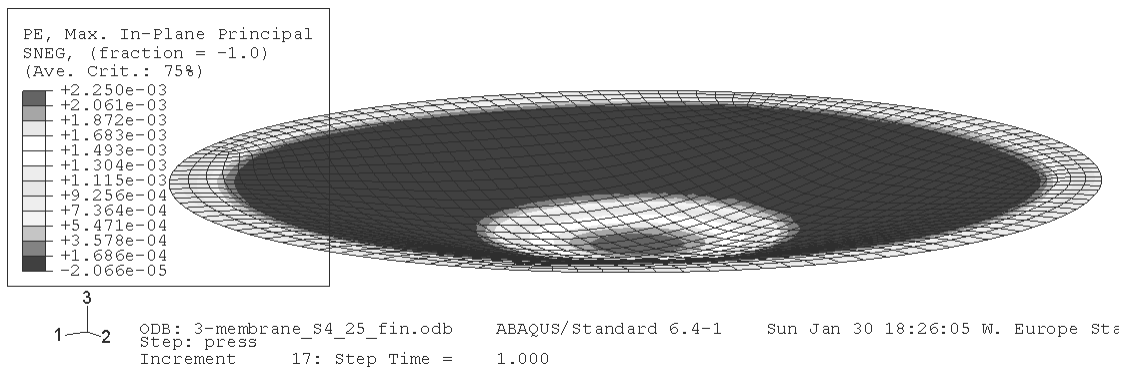


Figure 9. Plastic strain distribution.

The more detailed comparison of the results is presented in the following graphs (see Figure 10, Figure 11 and Figure 12). The simulated deflection of the membrane under load (1.5MPa) is shown in Figure 10. The results vary relatively much. The maximum deflection of the membrane according to the models 1 through 4 is between 34 $\mu$ m and 38 $\mu$ m. The 3D model results differ more (24 $\mu$ m). In Figure 10 the analytical solution for the deflection of the circular membrane is shown as well. The analytical solution assumes that membrane deforms purely elastically.

The simulated principal plastic strain distribution in the membrane under pressure is shown in Figure 11. The first, third and fourth models give similar distribution of plastic strain. Membrane deforms mostly in the centre and slightly close to the edge. According to the second model the membrane plastically deforms in a similar way but in a higher grade. This is in a good agreement with the deflection of the membrane described in the previous figure (Figure 10). The 2D-wire model indicated the highest grade of the membrane deformation.

The full scale 3D model indicates that membrane should deform along the edge only, letting the centre to deform elastically.

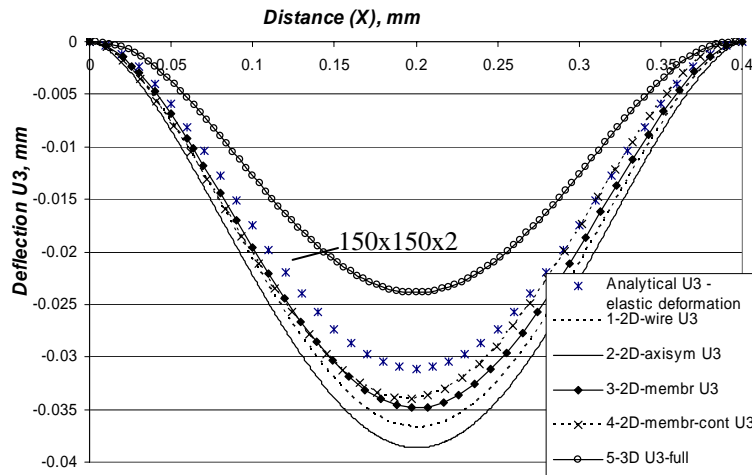


Figure 10. Simulated deflection of the membrane under pressure (1.5MPa – load sufficient for elasto-plastic deformation), membrane is glued to the substrate.

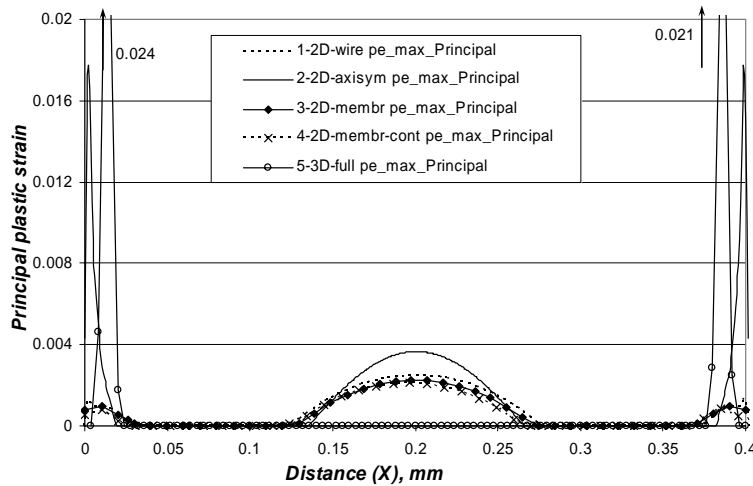


Figure 11. Simulated principal plastic strain distribution in the membrane under pressure (1.5MPa – load sufficient for elasto-plastic deformation), membrane is glued to the substrate.

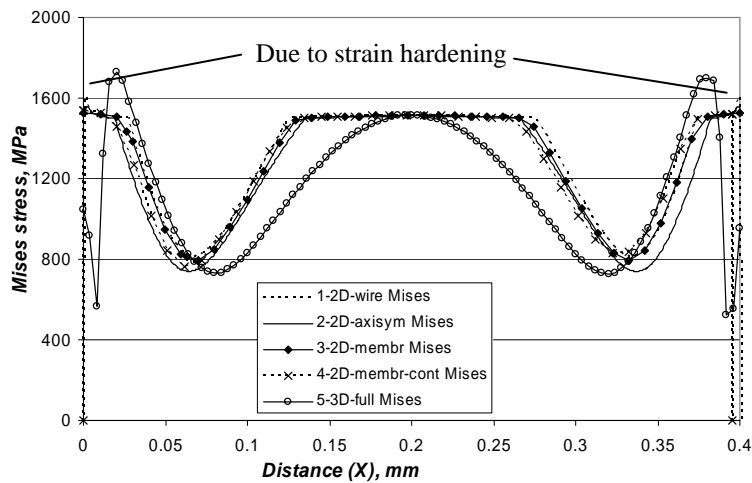


Figure 12. Simulated Mises stress distribution in the membrane under pressure (1.5MPa – load sufficient for elasto-plastic deformation), membrane is glued to the substrate.

In Figure 12 the Mises stress distribution in the membrane under pressure is shown. The 3D model indicates that in the centre the stress is almost reaches the limit (1.5GPa), while at the edges this limit exceeds the initial limit and grows further due to strain hardening included in the model. All the simplified models (1 through 4) form the flat area in the centre region of the graphs. The width of this region corresponds to the width of the area that reached the plastic state. Closer to the edge all the models indicate that the membrane should reach the yield stress limit.

#### 4.2 Elastic deformation

In order to study how the different models describe the elastic deformation of membrane a 10bar (1.0MPa) pressure was applied to the top surface of the membrane. Deformation of the membrane estimated according the models 1, 3 and 4 is coincides with the analytical solution very well. According to the 2-nd model (2D axisymmetric model) membrane should deform slightly more (about 5% disagreement). This difference is due to through-thickness stress distribution taken into account in this model.

The full scale 3D model gives quite conflicting results. The model where the part of the membrane with highest mesh density is meshed with 150x150x2 elements was used for comparison. Both 1-st and 2-nd order approximation elements were tested with full- and reduced integration.

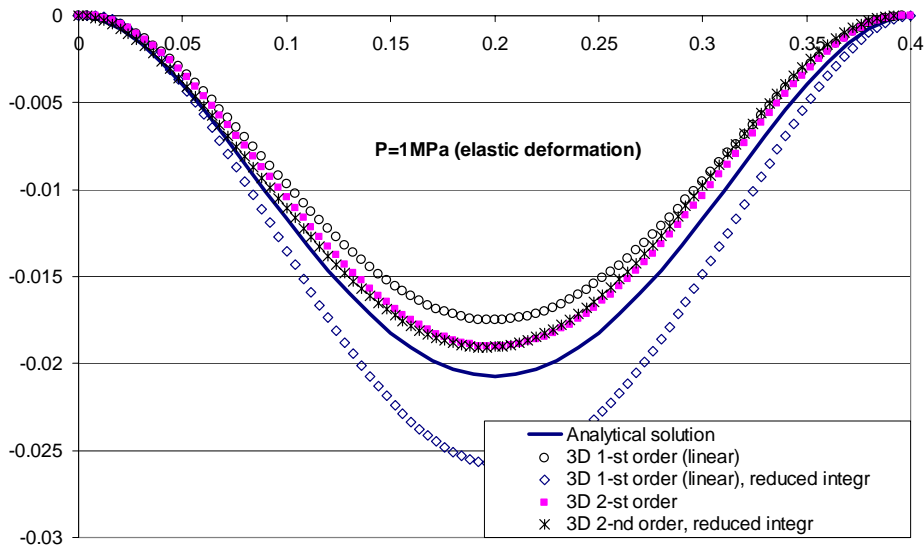


Figure 13. Simulated deflection of the membrane under pressure (1.0MPa – load sufficient for elastic deformation only), membrane is glued to the substrate.

The model with linear elements and reduced integration over predicted deformation by 25%, while the other models simulate deformation of the membrane by 8-15%.

#### 4.3 Mesh density effect

Controversial results acquired with 3D models prompted me to investigate the effect of the mesh density on resulting deformation of the membrane. These investigations were done for elasto-plastic loading (1.5MPa).

The shape of the used brick elements should be kept as close to cubic shape as possible in 3D model. Otherwise the predicted deformation of the membrane would be underestimated. It was proven to be true by sequential refinement of the mesh. These results are shown in Figure 14. The numbers along the 3D-model curve indicate the amount of elements in the most dense region of the mesh – central part of the membrane (see Figure 7).

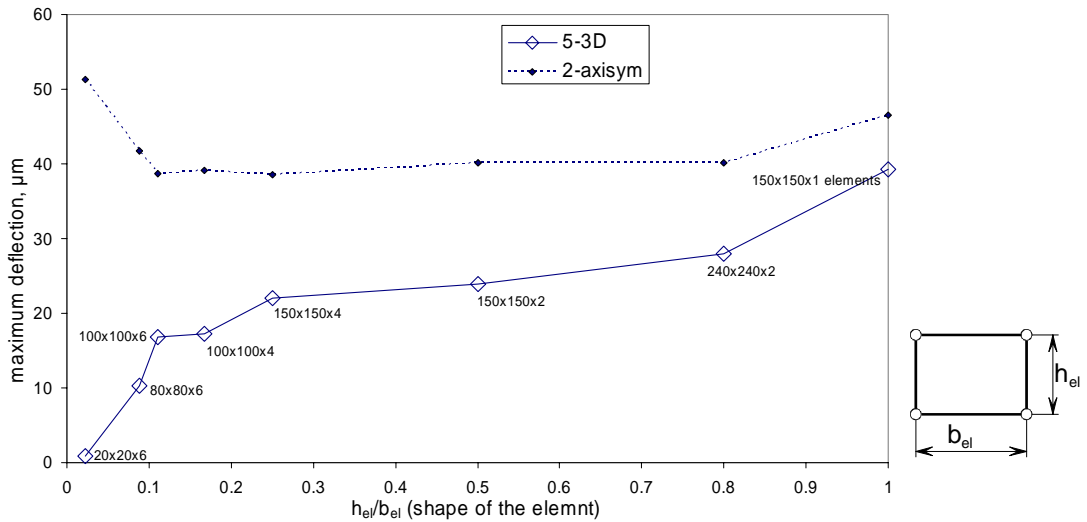


Figure 14. Effect of element shape and mesh density on the maximum deflection of the membrane under load.

The results for both full 3D model and the 2D-axisymmetric model are shown in Figure 14. It is obvious that 2D-axisymmetric model is not very sensitive to element shape and density, while 3D model gives the results varying quite significantly (between 0.8 $\mu\text{m}$  and 40 $\mu\text{m}$ ) with changing mesh parameters.

#### 4.4 The effect of gluing

Two opposite types of the tangential behaviour were tested. In one case the contact surfaces were allowed to glide without any friction in the other case the bodies were assumed to be glued to each other (in ABAQUS nomenclature it is called “tie”). Gliding allows more material to be “fed” into the hole from the adjacent area due to elastic elongation of the membrane surrounding the hole in the substrate, and by these means allowing more extensive deflection of the membrane (see Figure 15).

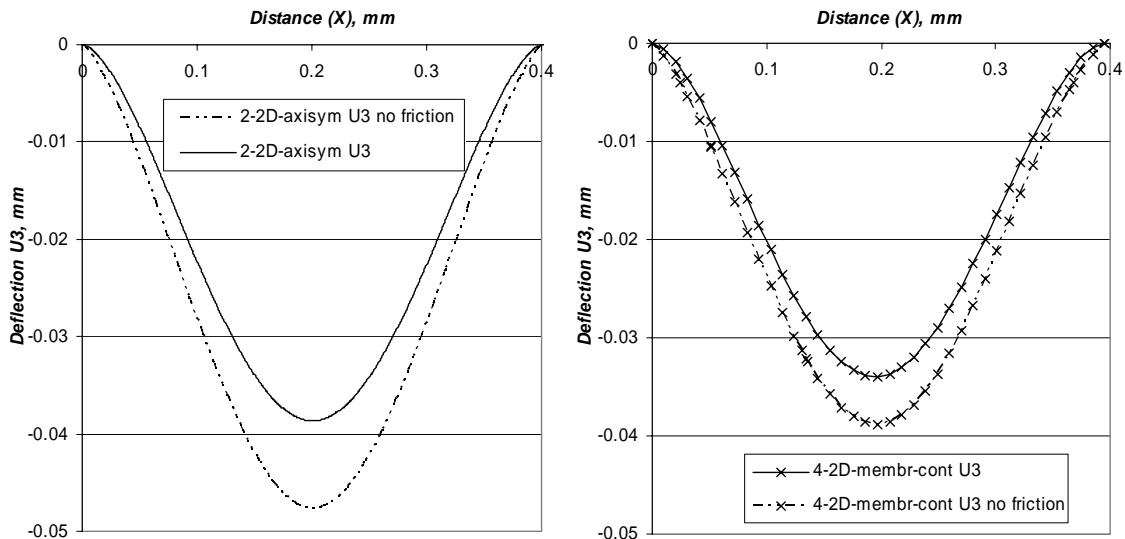


Figure 15. Effect of definition of the contact between membrane and substrate; (a) – 2D axisymmetric case; (b) – 3D-membrane case.

## 5. Conclusions

The full 3D modelling approach would not be advised for the applications similar to those under consideration of this paper. It is due to highly disproportional geometry – the membrane is much larger in the lateral direction than its thickness.

From the four simplified models the 2D-axisymmetric model can be recommended for further inverse modelling due to its robustness and appropriate approximation of the real phenomenon. This model takes into account the through-thickness distribution of the stress-strain fields which in its turn is important for the accurate prediction of the membrane deformation under pressure.

Depending on the level of friction force between the membrane and the substrate in the experiment the model with or without contact analysis should be chosen. The 2D and 3D-shell models even with contact analysis discussed in this paper, are relatively simple for the today's computers. Hence, the models where the substrate is modelled by the rigid body and not by the simple constraining of the edges are preferable.

Further investigation of the full scale 3D model in order to determine the reason for existence of the observed controversial results is recommended.

## References

- 1 R. Ramachandran and R.K. Menon. “*An Overview of Industrial Uses of Hydrogen*”. Int. J. Hydrogen Energy, 23, 593 (1998);
- 2 B.H.C. Steele and A. Heinzl. “*Materials for Fuel–Cell Technology*”. Nature, 414, 338, (2001);
- 3 Fraunhofer Institut Solare Energiesysteme. “*Environmentally Friendly Power Supply with Hydrogen*”. Press Release. Freiburg March 30, (2004) No. 03/04;
- 4 F.A. Lewis. “*The Palladium Hydrogen System*”. Academic Press (1967);
- 5 F.A. Lewis. “*Hydrogen in Palladium and Palladium Alloys*”. Int. J. Hydrogen Energy, 21, 461 (1996);
- 6 S.Timoshenko and S. Woinowsky-Krieger. “*Theory of plates and shells*”. McGraw-Hill. 2-nd Edition (1959). p.54.
- 7 ABAQUS v.6.4. *ABAQUS user's manual*. Vol.1. Providence, Rhode Island, USA (2004)